Modeling of High-Temperature Ceramic Membranes for Oxygen Separation

J.M. Gozálvez-Zafrilla[*,1], J.M. Serra[2], A. Santafé-Moros[1]
[1]Chemical and Nuclear Engineering Depart. Universidad Politécnica de Valencia (UPV)
[2]Instituto de Tecnología Química (UPV-CSIC)
*C/Camino de Vera s/n 46022 Valencia (Spain), jmgz@iqn.upv.es

Abstract: Oxygen transfer through ceramic membranes at high-temperature can substantially reduce costs respect to conventional separation methods. With the aim to improve the determination of the properties of the ceramic materials, a lab-scale permeation set-up was modeled using the Chemical Engineering module of COMSOL Multiphysics. The solution required the coupling of three domains (permeate compartment, air compartment and membrane). Gas flow was laminar and it was modeled using the Navier-Stokes equations. Oxygen transport was modeled using the convection and diffusion mode, Maxwell-Stephan diffusion, and diffusion of oxygen vacancies which is the relevant transport mechanism in the membrane. The boundary conditions at the membrane interfaces included the equilibrium between the oxygen in the gas and the concentration of its vacancies in the membrane and equal oxygen fluxes at both sides of each interface. The model was used to perform a parametric study of the geometry and to adjust the vacancy diffusion coefficient that produced a better approximation to the experimental results.

Keywords: ceramic membranes, oxygen separation, Maxwell-Stefan diffusion, vacancy transport.

1. Introduction

Oxygen separations by membranes are an interesting alternative to the cryogenic methods. Membrane separations will make possible to reduce energy requirements and investment cost. Moreover, they can be thermally integrated in *oxyfuel* power plants and make possible to match the desired oxygen production due to the intrinsic modularity of these systems. Apart from usual applications of oxygen in several industries, e.g. steel industry or petrochemistry, membranes are able to achieve high grade purity (theoretical selectivity of 100%) extending its possible applications.

Such a high selectivity can be achieved because oxygen separation is based on the transport of oxygen-ion vacancies through the lattice of a crystalline mixed oxide material (section 2). The most usual oxygen-ion conducting materials are based on the perovskite structure (ABO_3) and comprise Fe/Co/Ni and mixtures of lanthanide and alkali-earth metals in suitable proportions.

The development of these materials requires permeation studies at high temperature which are usually carried out in lab-scale permeation set-ups. In these experimental set-ups, typically, an averaged effective coefficient transfer through the membrane is obtained by measuring the oxygen transferred to a sweep gas stream. However, the value obtained depends on the geometry of the rig because of the following reasons:

- The oxygen concentration on each membrane side lacks uniformity and it differs from that of the bulk.
- The area placed under the seal contributes less to the oxygen transport than the rest of the membrane.

Another issue is that the oxygen transport mechanism in the membrane is due to vacancy diffusion, rather than current molecular oxygen diffusion. In the typical approach, the effective diffusion coefficient is directly calculated from oxygen pressure at both sides bypassing the equilibrium between oxygen pressure and concentration of oxygen vacancies. However, it would be more representative of the membrane properties to calculate a vacancy diffusion coefficient by means of the known gas molecules – vacancy equilibrium.

Our aim is to study the influence of the geometry and the experimental conditions and to obtain the true diffusion coefficient using the model by finding the value that matches better experimental results. The model obtained could be applied to design industrial ceramic modules using the vacancy diffusion coefficient.

2. Experimental set-up and

In the studied set-up (Figure 1 and 2), the membrane to be characterized is placed between two gas compartments; one circulated by air or oxygen and the other by a sweep gas (He or Ar). An averaged oxygen flux is measured for the entire membrane sample by analysis of the oxygen passed to the sweep gas. The concentration gradients through the membrane obtained by simulation are of great interest to determine the local diffusion coefficient of oxygen through the membrane.

Figure 1. Schematics of the experimental set-up.

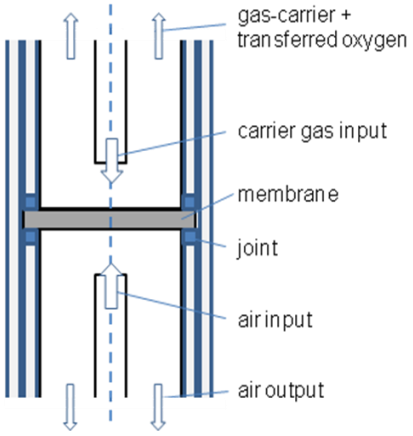

Figure 2. Experimental set-up (detail).

In the experiment used to evaluate the model, we used a membrane disc with diameter of 15 mm and thickness of 0.75 mm. The material was an oxygen deficient perovskite ($La_{1-y}Sr_yFeO_3$). The experiment was conducted at 1000ºC. The flow of gas to be separated (O_2=21%, N_2=79%) was 50 mL/min (measured at 25ºC). Same flow was established for the sweep gas (helium).

2. Oxygen transport through ceramic membranes

The most studied ceramic membranes to separate oxygen at high temperature are perovskite membranes. The generic chemical formula for a perovskite is $A_{1-y}A'_yBO_3$, where usually A = La; A' = Ca or Sr and B = Cr, Fe, Co or Mb.

The point defect model indicates that there is a relationship between the partial pressure of oxygen and the vacancy concentration in a structure with oxygen non-stoichiometry. The diffusion of oxygen is explained by the Wagner's theory through a mechanism that considers vacancy diffusion and the electronic transport together. There are two cases of non-stoichiometric materials: oxygen deficient perovskite and oxygen excess perovskite.

For the oxygen deficient perovskite that we used in the experiments, we have the following reactions:

- Defect reaction:

$$2\,Fe^{4+}_{Fe3+} + O^{2-}_{O} \leftrightarrow\ 2\,Fe^{3+} + V_O + \tfrac{1}{2}\,O_{2(g)}$$

- Disproportionation reaction:

$$2\,Fe^{3+} \leftrightarrow Fe^{4+}_{Fe3+} + Fe^{2+}_{Fe3+}$$

where Fe^{4+}_{Fe3+} and Fe^{2+}_{Fe3+} are a Fe^{+4} or Fe^{+2} formed in a Fe^{+3} position, and V_O is an oxygen vacancy.

For these reactions, we have the following equilibrium constants:

$$K_2 = \frac{\left[Fe^{3+}\right]^2 \cdot [V_O] \cdot p_{O2}^{1/2}}{\left[Fe^{4+}_{Fe^{3+}}\right]^2 \left[O^{2-}_{O}\right]}$$

$$K_3 = \frac{\left[Fe^{4+}{}_{Fe^{3+}}\right] \cdot \left[Fe^{2+}{}_{Fe^{3+}}\right]}{\left[Fe^{3+}\right]^2}$$

These equations can be combined with the electroneutrality condition and mass balances for the species that suffers disproportionation to obtain an equilibrium relationship between oxygen pressure in the gas and vacancy concentration in the solid. As the calculation is rather time-consuming, the vacancy concentrations were previously calculated for a number of pressures to create an interpolation function. To do so, the following values of equilibrium constants at 1000 ºC provided by Bart et al. (Ref. 1) were used: $K_2 = 7 \cdot 10^{-2}$ atm$^{1/2}$ and $K_3 = 1 \cdot 10^{-6}$. Fig. 3 shows the results obtained.

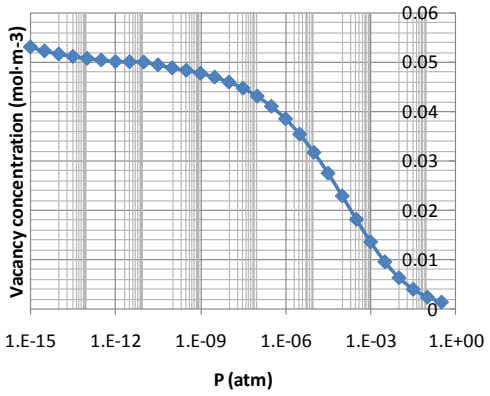

Figure 3. Calculated equilibrium between oxygen in the gas and oxygen vacancies in the solid.

3. Modeling

The three subdomains of the model were: 1: permeate, 2: membrane, 3: oxygen/nitrogen mixture. Oxygen is transferred from subdomain 3 to subdomain 2 and from the latter to subdomain 1. It was necessary to solve gas flow, oxygen diffusion and vacancy diffusion.

3.1 Governing equations

Flow in subdomain 1 was laminar at the conditions used in the experiment. It was modeled using the Incompressible Navier-Stokes mode. In the permeate phase the oxygen is at very low concentration, so its concentration could be modeled using the Convection and Diffusion mode of the Chemical Engineering module.

For subdomain 3 the flow was also laminar, so the Incompressible Navier-Stokes was also applicable. However, in this phase, oxygen has high proportion in the mixture, therefore, the Maxwell-Stefan Diffusion and Convection (Chemical Engineering module) is the right choice. In this case, the oxygen diffusion is coupled with the gas flow as it affects the density of the fluid.

For the membrane, we used the vacancy diffusion instead of an equivalent oxygen diffusion to have a model approach near to the physical reality.

The different model equations and the state variables are summarized in Table 1. For the sake of conciseness, we refer to (Ref. 2) for a detailed description of the equation set.

Table 1: Equations used for each subdomain

Subdomain	Equations	Variables
1 (sweep gas + O_2)	Incompressible Navier-Stokes + Continuity (*chns*)	u, v, p
	Convection and Diffusion (*chcd*)	C
2 (membrane)	Diffusion (*chdi*)	o
3 (N_2 + O_2)	Incompressible Navier-Stokes + Continuity (*chns*)	u3, v3, p3
	Maxwell-Stefan Diffusion and Convection (*chms*)	w1

3.2 Properties

As the main component in the permeate phase is the sweep gas helium, the properties of this gas at 1000 ºC were used in the Incompressible Navier-Stokes mode:

ρ=0.038314 kg/m^3, $\mu = 4.3\times10^{-5}$ Pa·s.
The oxygen diffusion in helium was 9.11×10^{-4} m^2/s.

In subdomain 3, the gas density depends on the composition. To obtain the gas density from the oxygen mass fraction, the following subdomain expression was added:

$$\rho = \frac{p}{R_g \cdot T}\left[\frac{w_{O2}}{M_{O2}} + \frac{(1-w_{O2})}{M_{N2}}\right]^{-1}$$

The Maxwell-Stefan diffusivities for the mixture of nitrogen and oxygen were described with the following empirical equation (Ref. 3) based on the kinetic gas theory:

$$D_{O2,N2} = \frac{k_d \cdot T^{1.75} \cdot \left(M_{O2}{}^{-1} + M_{N2}{}^{-1}\right)^{1/2}}{p \cdot \left(v_{O2}{}^{1/3} + v_{N2}{}^{1/3}\right)^2}$$

where $k_d=3.16\cdot10^{-8}$ Pa·m^2·s^{-1}, and the molar volumes are $v_{O2}=1.66\times10^{-5}$ mol/m^3 and $v_{N2}=1.79\times10^{-5}$ mol/m^3.

3.3 Geometry and boundary specifications

Subdomains were drawn in separate geometries that were 2D axis-symmetrical. Figure 4 shows the three geometries at the same time. Gas inlets appear in blue color and outlets in green colour.

In the first approach, the dimensions of subdomain 3 were those of the set-up. However, the first fluid dynamics calculations indicated that the flow was almost stagnant in the most part of the tube. Therefore, the lower part of the geometry was cut out and substituted by a slip boundary condition at the bottom.

For subdomains 1 and 3, the boundary conditions for the incompressible Navier-Stoke mode were the following: gas inlets used a laminar inflow b.c.; outlets were set at the pressure of the system (p = 101300 Pa); for the axis, axial symmetry b.c. was used; the rest of the boundaries used non-slip b.c (except the bottom of subdomain 3).

For subdomains 1 and 3, the boundary conditions for the Convection and Diffusion mode and Maxwell-Stefan Diffusion were: inlets set at the corresponding oxygen concentration of the entering gas, outlet at convective flow, axis used axial symmetry, the rest used an insulation b.c. except the limits with the membrane that used coupled b.c. with the membrane subdomain.

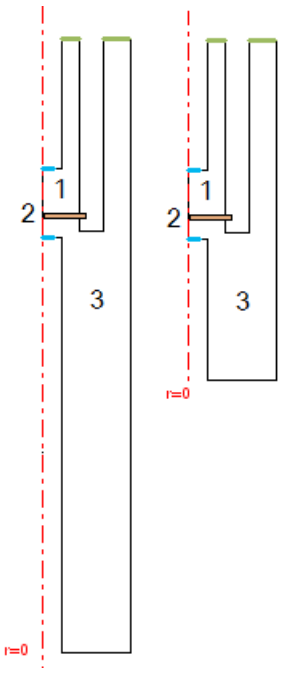

Figure 4. Initial geometry and cut-out geometry.

3.4 Coupled boundary conditions

The definition of the boundary condition at the membrane interfaces required the coupling of variables between the connected subdomains.

The interpolation function *Vo* that depends on the logarithm of the oxygen pressure (in atm) was used to build identity b.c.'s to define the vacancy concentration in the membrane from the molar oxygen concentration of subdomain 1 or the mass oxygen concentration of subdomain 3.

The identity between the flux of oxygen and the vacancy flow at the upper interface was established by defining the following boundary extrusion coupling variables:

```
flux12 = -2*ndflux_c_chcd
flux21 = -0.5*ndflux_o_chdi
```

Afterwards, these variables were included in the boundary definition of the gas (flux21) and the membrane (flux12) sides.

Similarly, for the lower interface, the following extrusion variables were defined and used in the boundary definition:

flux23 = -2*ndflux_o_chdi*M_O2
flux32 = -0.5*ndflux_w1_chms/M_O2

The coefficient multiplying the flux reflects the stoichiometry between the oxygen flux (molar or mass) and the flux of vacancies. The negative sign appears due to the different direction of the oxygen and vacancy flux.

3.5 Meshing

Figure 5 shows a detailed of the meshes performed for each geometry. Interactive meshing was use to refine the mesh in the zones with higher gradient concentration of oxygen or abrupt changes of flow direction.
The number of mesh elements were 32372, 392 and 2502 respectively for subdomains 1, 2 and 3.

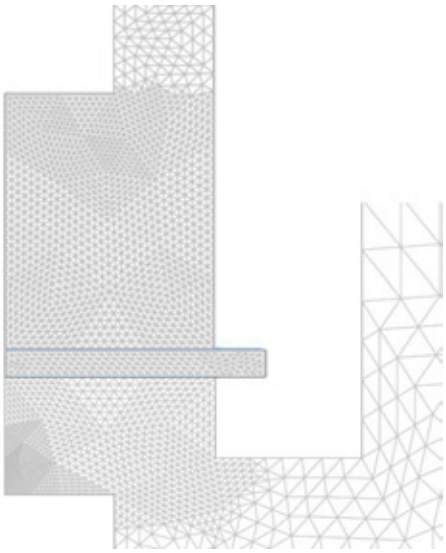

Figure 5. Meshes performed in the three geometries.

3.6 Solver used

The solver used was the stationary solver UMFPACK. Starting from the scratch, the flow was previously solved for subdomains 1 and 3 without considering permeation (that is at constant gas composition). The solution obtained was the initial solution for the coupled problem.

4. Results

The vacancy diffusion coefficient in the material is a model input, which is not previously known, but could be obtained by comparing model results with experimental data. Once this coefficient was obtained, a parametric study of the influence of the geometry and entering flow could be performed. The coefficient is important as a measure of the performance of the material and for design purposes.

4.1 Fitting of the vacancy diffusion

For the experimental conditions indicated in section 2, the average oxygen flux through the membrane obtained experimentally was
$J = 5 \cdot 10^{-4}$ mol·m^{-2}·s^{-1}

To find the vacancy diffusion coefficient (D_{vo}) that corresponded to this value, a quadratic interpolation technique was applied as follows:

1) For three guessed values of D_{vo}, the model is run to obtain the corresponding fluxes and consequently three pairs of the form ($D_{vo,guessed}$, J).
2) A quadratic polynomial is fitted to the points and the value of $D_{vo,int}$ that gives the desired J in the function is found.
3) The model is applied to calculate the value of J for $D_{vo,int}$. The solution of the nearest $D_{vo,gessed}$ can be used as initial value.
4) The points with values of $D_{vo,guessed}$ nearer to $D_{vo,int}$ are preserved with the latter for a new iteration.

The procedure converged after two additional iterations (5 total calculations) yielding a value of $D_{vo} = 16.7 \times 10^{-5}$ m^2·s^{-1}.

Figure 6 shows the molar concentration of oxygen in subdomain 1, and Figure 8 the mass fraction of oxygen obtained for the converged D_{vo}. Figure 7 shows the distribution of oxygen vacancies. Note the high vacancy concentration at the permeate side of the membrane compared to the feed side, what is consistent with the oxygen-vacancies equilibrium.

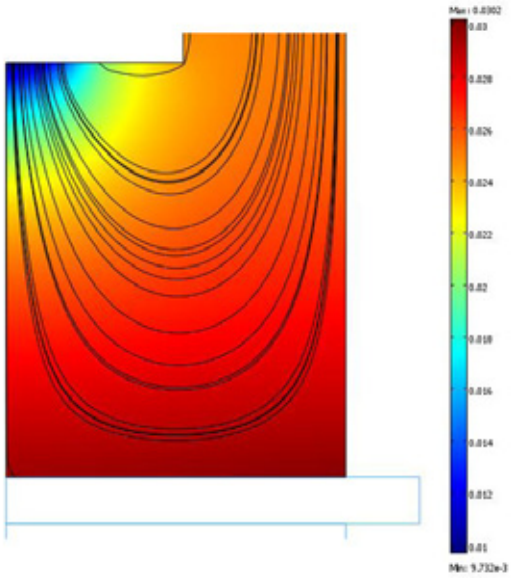

Figure 6. Molar concentration of oxygen (mol/m^3) and flow streamlines in subdomain 1.

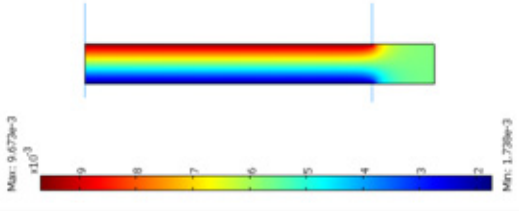

Figure 7. Vacancy concentration in subdomain 2.

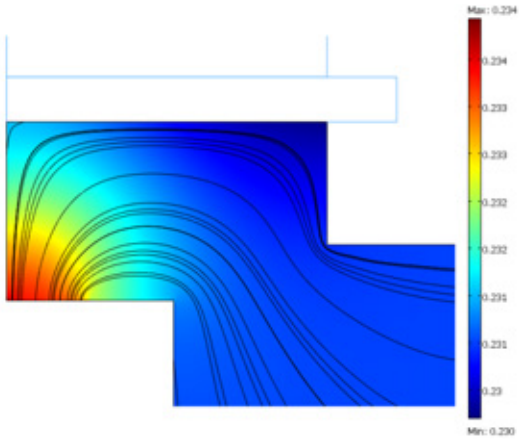

Figure 8. Mass fraction of oxygen and streamlines in subdomain 3.

4.2 Parametric studies

The results showed a lack of homogeneity for the oxygen concentration on the membrane interface (Figure 9). This causes a variation of flow along the r-coordinate. In Figure 10, we can see the effect of varying the flow of sweep gas and air on the flux of vacancies. We can see that the effect of the seal in the profiles is important and, as a consequence, it should not be neglected to calculate the average diffusion coefficient.

Figure 11 shows the effect of approaching the gas inlet to the membrane. It can be seen that the near the position, the less homogeneous the concentration on the membrane.

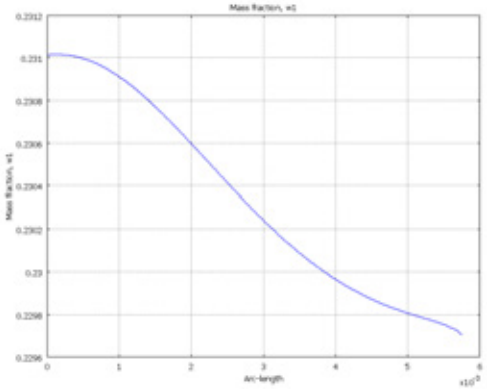

Figure 9. Mass fraction of oxygen at the membrane interface.

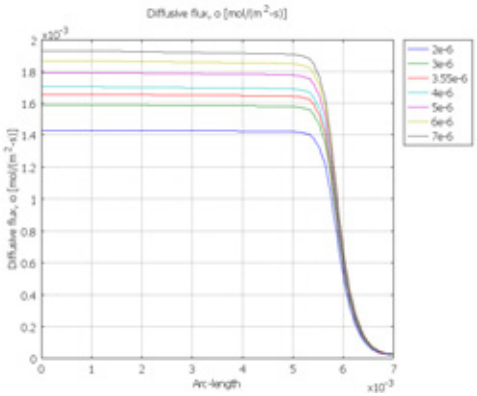

Figure 10. Flow of oxygen vacancies in the medium cross section of the membrane for different values of gas flow.

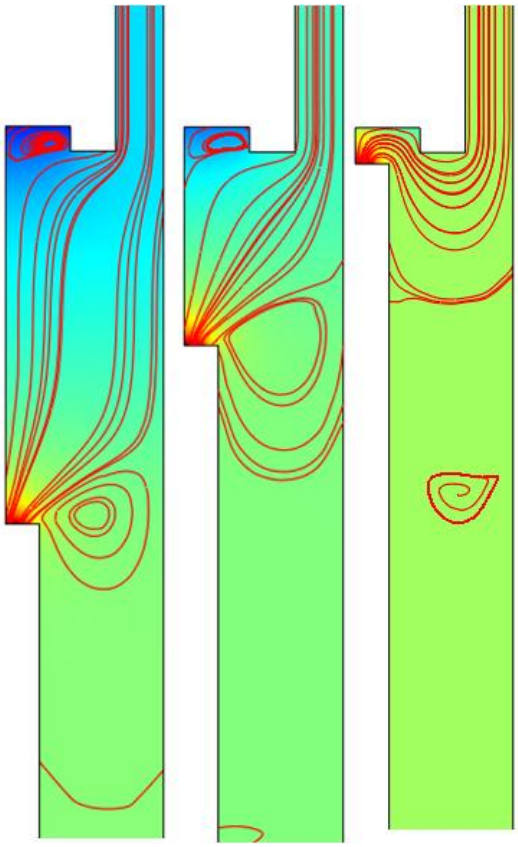

Figure 11. Oxygen concentration for three different positions of the gas inlet.

5. Conclusions

A model to study the transfer of oxygen through a ceramic membrane has been developed.

The model was used to obtain the value of the diffusion coefficient of vacancies of oxygen in the membrane materials, which is important to develop this type of materials and to design to design industrial ceramic modules. The model was also used to study the effects of experimental conditions and geometry on the performance of the characterization set-up.

6. Acknowledgements

The Spanish Ministry for Science and Innovation (Project ENE2008-06302) and the Consellería d'Educació de la Generalitat Valenciana (Project GVPRE/2008/334) are kindly acknowledged.

7. References

1. Bart, A. van Hassel et al., Oxygen permeation modelling of perovskites, *Solid State Ionics*, **66**, 295-305 (1993)
2. COMSOL AB, *Chemical Engineering Module User's Guide*, 118-256, (electronic document) (2008)
3. J. A. Wesselingh and R. Krishna, *Mass Transfer in Multicomponent Mixtures*, Delft University Press (2000).